Preprint
UCRL-JC-139496

Advanced Model for SBS of a Randomized Laser Beam and Application to Polarization Smoothing Experiments with Preformed Underdense Plasmas

V.T. Tikhonchuk, J. Fuchs, C. Labaune, S. Depierreux, H.A. Baldis, S. Hüller, J. Myatt and D. Pesme

U.S. Department of Energy

Lawrence
Livermore
National
Laboratory

This article was submitted to
ECLIM 2000 XXVI European Conference on Laser Interaction with Matter
Prague, Czech Republic
June 12-16, 2000

June 30, 2000

UCRL-JC-139496

Advanced model for SBS of a randomized laser beam and application to polarization smoothing experiments with preformed underdense plasmas

V. T. Tikhonchuk[a,b], J. Fuchs[a], C. Labaune[a], S. Depierreux[a], H. A. Baldis[c,☨], S. Hüller[d], J. Myatt[d], and D. Pesme[d]

[a] Laboratoire pour l'Utilisation des Lasers Intenses, École Polytechnique, 91128 Palaiseau, France

[b] P. N. Lebedev Physics Institute, Russian Academy of Science, 117924 Moscow, Russia

[c] Institute for Laser Science and Applications, Lawrence Livermore National Laboratory, Livermore, CA 94550, USA

[d] Centre de Physique Théorique, École Polytechnique, 91128 Palaiseau, France

ABSTRACT

An advanced statistical model is presented, which describes the SBS of a randomized laser beam interacting with an underdense, expanding plasma. The model accounts for the self-focusing of speckles and for its influence on the speckles SBS reflectivity in the regime where the effect of plasma heating is important. Plasma heating has an important effect on speckle self-focusing and it decreases the SBS threshold and also decreases the SBS reflectivity. The model exhibits a good agreement with the measured SBS levels at the LULI multi-beam facility for a broad range of the laser and plasma parameters and both types of beam smoothing – RPP and PS. Both the model and the experiments confirm that the PS technique allows to control the SBS level more efficiently than RPP.

Keywords: Stimulated scattering, laser speckle, self-focusing, collisions, ponderomotive force, randomized beam.

1. INTRODUCTION

The stimulated Brillouin scattering (SBS) plays an important role in the laser plasma interaction because it may reflect a significant part of the laser energy and degrade the laser coupling to the target in the ICF conditions. A significant progress in understanding the SBS has been achieved when it has been recognized that the SBS is originating in high intensity speckles of the laser light,[1] and a SBS model has been developed[2,3] that accounts for speckle statistics, self-focusing of the laser light in speckles, and for the convective SBS amplification and saturation. The statistical SBS model has already demonstrated a good agreement with the experiments.[4] In the present formulation we account for recent achievements in the theory of nonlocal plasma transport and laser speckle statistics and incorporate them in the model. Plasma heating makes a significant impact on the SBS: it results in a lower threshold for the SBS excitation and also in a deeper density depletion which saturates the SBS reflectivity at a lower level. This advanced model demonstrates much better agreement with experimental data on the SBS reflectivities, time history of the backscattered signal, and the spatial location of the SBS activity for different laser intensities, smoothing techniques, and plasma targets.

2. SBS FROM SELF-FOCUSED SPECKLES

2.1. Model for the speckle self-focusing

The model described below is an extention and amelioration of the model for the SBS reflectivity from the ponderomotively self-focused speckles described in.[2,3] It is based on an assumption that each representative speckle is in a stationary state, that is, the self-focused speckle is stable and the characteristic time of variation of laser and plasma parameters is longer than the self-focusing time, a_0/c_s, and the time of SBS saturation, l_a/c_s. Here, c_s is the ion acoustic velocity, a_0 is the speckle radius, $l_a = \nu_a L_v$ is the SBS convective amplification length, $\nu_a = \gamma_a/\omega_a$ is the normalized ion acoustic wave damping, and $L_v = c_s/(du/dz)$ is the inhomogeneity length of the plasma expansion velocity, $u(z)$. For the typical parameters: $\nu_a = 0.1$, $a_0 = 3\,\mu$m, $l_a = 5\,\mu$m, and $c_s = 0.2\,\mu$m/ps, the equilibration time is about 25 ps, which is short compared to the laser pulse and plasma evolution time ~ 400 ps.

☨ Institute for Laser Science and Applications (ILSA), Lawrence Livermore National Laboratory, Livermore, California 94550

The propagation of laser light in a speckle is described in the paraxial approximation and assuming that the laser electric field keeps approximately Gaussian shape, $E = a^{-1}\sqrt{P/\pi}\exp[-(r/a)^2 + i(k_0 r^2/2a)\, d_z a + i\psi]$, The beam power P is conserved in the present description and the equation for the beamlet radius $a(z)$

$$k_0^2 a^3 d_z^2 a = 1 + 2\,(\omega_{pe}/c)^2 \int_0^\infty r dr\,(1 - r^2/a^2)\,(\delta n/n_e)\,\exp(-r^2/a^2)\,, \tag{1}$$

has been derived by taking the radial moments of the paraxial wave equation. This method of moments agrees exactly with the variational method[3] for the case of ponderomotive nonlinearity and it is also in much better agreement with the numerical simulations than the paraxial ray method. The density perturbation in the speckle, δn, is defined by a combined action of the ponderomotive and thermal nonlinearities:

$$\delta n(r)/n_e = -3.72p\,(c/\omega_{pe})^2 \int_0^\infty k\,dk\,A(k\lambda_{ei}) J_0(kr)\,\exp\,(-k^2a^2/4)\,, \tag{2}$$

where ω_{pe} is the electron plasma frequency, J_0 is the zero-th order Bessel function, $p = P/P_c$ is the ratio of the beamlet power to the critical power for the ponderomotive self-focusing, and the function A accounts for the ponderomotive and thermal effects on the plasma density: $A = 1/2 + 0.88Z^{5/7}(k\lambda_{ei})^{-4/7} + 2.54Z/[1 + 5.5Z(k\lambda_{ei})^2]$.[5] The temperature perturbations can be represented in the similar way as Eq. (2) with the function A substituted by $A_T = -1/3 - 0.91Z^{5/7}(k\lambda_{ei})^{-4/7}$, which accounts for the heat transport from the speckle.

Equation (2) and the similar equation for the temperature perturbation are valid for $|\delta n| \ll n_e$ and $|\delta T| \ll T_e$. We extrapolate these formulae to finite amplitude perturbations with two modifications: (i) we introduce the exponential saturation of the density perturbation, $n(r)/n_e = \exp(\delta n/n_e)$, and (ii) we accont for an increase of the electron mean free path due to the density depletion and temperature increase in the speckle: $\bar{\lambda}_{ei} = \lambda_{ei}(1 + \xi\delta T(0)/T_e)^2/\exp(\xi\delta n(0)/n_e)$. Then we solve Eq. (2) and the similar equation for δT for on-axis density and temperature perturbations, and the renormalized electron mean free path has been used then in Eq. (1) in calculations of the integral in the right hand side. The empirical coefficient ξ is considered as a free parameter. It affects the depth of the density channel and the level of SBS reflectivity. We define this coffecient, $\xi \approx 0.5$, by matching the calculated SBS reflectivies to the experimental data.

2.2. Single-speckle SBS reflectivity

The equation for the SBS power, P_B, has been derived in[2] with assumption that the three-wave SBS interaction length, l_a, is shorter than the characteristic length of the intensity variation along the speckle axis: $d_z P_B = -\epsilon\,\Delta\Omega(\beta)\,\exp 2G_B$, where ϵ is the effective noise level and $\Delta\Omega$ is the effective angle of the SBS emission. In the present formulation we account for the intensity variation within the SBS interaction length, which may occur in the regime of strong self-focusing: the SBS gain G_B and the parameter β were integrated over the resonance length. For example, $G_B(z) = \int dz' g_B(z')/[1 + (z - z')^2/l_a^2]$, where $g_B = \gamma_0^2/\gamma_a|V_s|$ is the local SBS spatial growth rate which includes the effects of density inhomogeneity, intensity enhancement, local heating, and the density depletion. The dependence of SBS emission angle on β is described in,[3] and the parameter β is defined by a similar formula with g_B in the right hand side substituted by $\sqrt{g_B/k_0 a^2}$.

The SBS reflectivity, $R_B(P)$, has been calculated for a given input power P after Eq. (1) has been solved and the axial dependence of the speckle radius, $a(z)$, was known. The dependence of the SBS reflectivity on the speckle power is shown in Fig. 1a for a weakly collisional case, $a_0/\lambda_{ei} \approx 0.5$ for f-number 6 and 0.25 for $f = 3$. The cases of the ponderomotive self-focusing and the SBS without self-focusing are shown for comparison. There are two effects associated with the thermal nonlinearity: (i) the threshold of self-focusing (and the SBS threshold, correspondingly) is reduced due to the speckle heating as compared to the ponderomotive case, and (ii) above the self-focusing threshold the level of SBS reflectivity is reduced because of much stronger density depletion and temperature enhancement in the speckle. It is important to notice that the full model demonstrates a weak dependence on f-number, which is not the case for the reduced models.

2.3. Macroscopic SBS reflectivity

The local macroscopic backscattering reflectivity, is defined as an ensemble average of a single-speckle reflectivity, assuming that all speckles are independent. According to,[2] $\langle R\rangle$ describes an increase of the SBS intensity at one Rayleigh length, $L_R = k_0 a_0^2$: $\langle R\rangle = \int u du\, f(u) R_B(\pi a_0^2 \langle I\rangle u)$, where $\langle I\rangle$ is the local average laser intensity. The

limits of integration, $u_{min} = 1.5$ and $u_{max} = 10$, where chosen in such a way that they do not affect the result in the parameter range we considered. The speckle distribution function was taken from.[6] For the RPP beam: $f_{RPP}(u) \approx 0.95u^{3/2}e^{-u}$. For the case of polarization smoothing (PS), which corresponds to overlapping of two RPP fields of a half of average intensity and orthogonal polarizations, $f_{PS}(u) = 2f_{RPP}(2u)$. A relation between the radius of the Gaussian beamlet introduced in Sec. 2.1 and the laser beam f-number was chosen in such a way that the Gaussian speckle has the same power and the same maximum intensity as the cylindrical flat-top RPP speckle used in[6]: $a_0 = (2/\pi) f\lambda_0$.

A typical dependence of the averaged SBS reflectivity on the plasma density and the laser intensity is shown in Fig. 1b. (The PS reflectivity demonstrates a similar behavior but it is always lower than the RPP reflectivity because there are less high intensity speckles in that case.) The SBS reflectivity exponentially increases with the density, while it clearly saturates as a function of the laser power, and it also demonstrates a very weak dependence on the beam f-number. These dependences are similar to what has been observed in the LULI experiments.

3. MODELING OF THE LULI EXPERIMENT

The equation for the average laser intensity accounts for the SBS and the inverse Bremsstrahlung (IB) absorption[4]: $d_z\langle I\rangle = -(\langle R_B\rangle/L_R + \kappa_{IB})\langle I\rangle$, where κ_{IB} is the IB absorption coefficient. The incident laser intensity has a Gaussian radial and temporal profile, $\langle I\rangle_{inc} = I_0 \exp(-t^2/t_{las}^2 - r^2/r_{las}^2)$ with $t_{las} = 335$ ps and $r_{las} = 125\,\mu$m for the $f/6$ beam. The plasma density depends exponentially on time, $n_{top}(t) = n_{max}\exp(-t/t_{plas})$ with $t_{plas} = 530$ ps, and has a bell-like profile in the direction of the laser beam propagation, $n_e = n_{top}/(1 + z^2/L_N^2 + z^4/L_N^4)$, where the parameter L_N could be a function of n_{top}. In the present model we use the following parametrization: $L_N(\mu\text{m}) = 500/[n_{top}/n_c + (n_{top}/n_c)^{0.27}]$, which is a numerical fit to the density profiles found in hydro simulations of plasma expansion. The plasma temperature was set to 600 eV for electrons and 300 eV for ions. The plasma expansion velocity depends linearly on the coordinate, $u = c_s z/L_v$, with a constant L_v taken from the experiment: $L_v = 120\,\mu$m for $n_{max} = 0.4n_c$, $200\,\mu$m for $0.2n_c$, and $280\,\mu$m for $0.1n_c$.

Using these parameters we calculated the density dependence of the total, space and time integrated SBS reflectivity for a given laser pulse energy and compared it with the observations in Fig. 2a. The results from reduced models (with the ponderomotive self-focusing and without any self-focusing) are shown also for comparison. It is evident that the thremal effects in self-focusing are important to explain the experiment. One can see two different slopes in the reflectivity dependence on the density which correspond to two different effects in the SBS saturation. Namely, the SBS is saturated due to the density depletion at low intensities, $n_{max} < 0.2n_c$, and due to the pump energy depletion for $n_{max} > 0.2n_c$.

The energy dependence of the integrated SBS reflectivity is shown in Fig. 2b for the case of $f/6$ RPP laser beam. The model is in agreement with observations for the whole range of studied energies. It explains the SBS threshold at the energy level of $5 - 10$ J. Non of other variants of the model is able to reproduce the experimental results. The ponderomotive self-focusing predicts about two times higher threshold and too high reflectivity above it. The SBS model without self-focusing predicts even higher threshold and very different dependence of the reflectivity on the laser energy. Similarly to what has been observed in the experiment, the model reflectivity weakly depends on the f-number for the same laser pulse energy and it also predicts a correct time evolution and spatial location of the SBS.

4. DISCUSSION

This comparative analysis illustrates that the present model incorporates the important elements of the SBS physics relevant for the parameters of the present experiments. The speckle self-focusing is required to explain the SBS at low beam energies and the ratio of SBS reflectivities for the RPP and PS beams. The thermal heating in a speckle further decreases the SBS threshold and it also enhances the density and temperature perturbations, which are the important factors for the early SBS saturation. Similar results have been obtained for the plasma with the maximum density at the peak of the laser pulse of 0.1 and 0.4 of the critical density and for the aluminum plasma. The thermal effects are also important for the plasma in NIF and LMJ targets. The electron density in hohlraums is about 10^{21} cm^{-3} and the electron mean free path is a few microns for the electron temperature of 3 keV in the CH plasma. The thermal effects are already important in such conditions, but they would be even more important in a high-Z plasma near hohlraum walls where the electron mean free path could be less than a tenth of micron.

This work was partially performed under the auspices of the U.S. Department of Energy by the University of California, Lawrence Livermore National Laboratory, through the Institute for Laser Science and Applications, under Contract No. W-7405-ENG-48.

REFERENCES

1. H. A. Rose and D. F. DuBois, "Laser hot spots and the breakdown of linear instability theory with application to stimulated Brillouin scattering," *Phys. Rev. Lett.* **72**, pp. 2883–2886, 1994.
2. V. T. Tikhonchuk, Ph. Mounaix, and D. Pesme, "Stimulated Brillouin scattering reflectivity in the case of a spatially smoothed laser beam interacting with an inhomogeneous plasma," *Phys. Plasmas* **4**, 2658–2669, 1997.
3. V. T. Tikhonchuk, S. Hüller, and Ph. Mounaix, "Effect of the speckle self-focusing on the stationary SBS reflectivity from a randomized laser beam in an inhomogeneous plasma," *Phys. Plasmas* **4**, 4369–4381, 1997.
4. V. T. Tikhonchuk, C. Labaune, and H. Baldis, "Modeling of a stimulated Brillouin scattering experiment with statistical distribution of speckles," *Phys. Plasmas* **3**, 3777–3785, 1996.
5. A. V. Brantov, V. Yu. Bychenkov, V. T. Tikhonchuk, and W. Rozmus, "Nonlocal electron transport in laser heated plasmas," *Phys. Plasmas* **5**, 2742–2453, 1998.
6. J. Garnier, "Statistics of the hot spots of smoothed beams produced by random phase plates revisited," *Phys. Plasmas* **6**, 1601–1610, 1999.

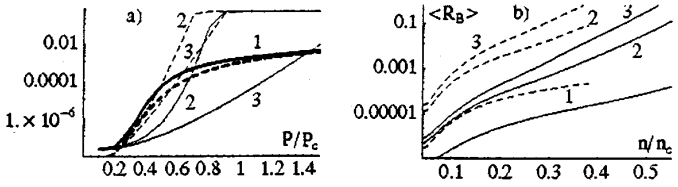

Figure 1. a) Dependence of the SBS reflectivity from a single speckle on the incident power (normalized to the critical power for the ponderomotive self-focusing). Dark lines (1) represent the result of the full model, which includes the ponderomotive and thermal self-focusing. Fine lines correspond to the case of ponderomotive self-focusing (2) or the case of SBS without self-focusing (3). Solid lines correspond to the case of $f = 6$, while dashed lines represent the case of $f = 3$. The parameters are typical for the LULI experiment: CH plasma with $n_e/n_c = 0.2$, $T_e = 600$ eV, $T_i = 300$ eV, $L_n = 800\,\mu$m, and $L_v = 200\,\mu$m. b) Dependence of the averaged SBS reflectivity on the plasma density for the $f = 6$ RPP beam and for different laser intensities normalized to the critical power for the ponderomotive self-focusing, $\langle p \rangle = \langle I \rangle \pi a_0^2 / P_c = 0.05$ (1), 0.2 (2), and 0.5 (3). Solid lines correspond to $L_v = 120\,\mu$m, while dashed lines correspond to $L_v = 200\,\mu$m. Other parameters are the same as in panel a.

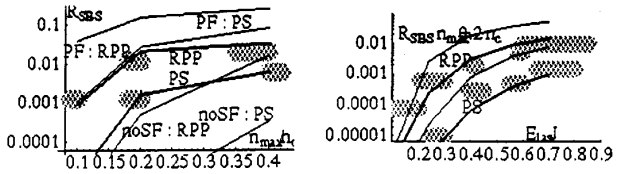

Figure 2. Model predictions and experimental results for dependence of SBS reflectivity on the plasma maximum density (a) and on the laser average intensity (b) for the $f/6$ RPP (1, 3, 5) and PS (2, 4, 6) beams. Dark lines 1 ans 2 correspond to the full model. Light lines $3 - 6$ are the predictions of the reduced models with the ponderomotive self-focusing (3, 4), and without self-focusing (5, 6). Shaded blocks are the experimental results for the CH plasma irradiated by the laser beam with the maximum average intensity 10^{14} W/cm^2 (a) and at the maximum density $n_{max} = 0.2 n_c$. Other parameters are described in the text.